Evidence for root adaptation to a spatially discontinuous water availability in the absence of external water potential gradients

CLASSIFICATION: BIOLOGICAL SCIENCES/PLANT BIOLOGY

Evidence for Root Adaptation to a Spatially Discontinuous Water Availability in the Absence of External Water Potential Gradients

Kara R. Lind[1, §], Oskar Siemianowski[1, §], Bin Yuan[2], Tom Sizmur[1‡], Hannah VanEvery[1†], Souvik Banerjee[1] Ludovico Cademartiri[1,2,3,4]*

[1] Department of Materials Science & Engineering, Iowa State University of Science and Technology, 3109 Gilman Hall, Ames, IA, 50011

[2] Department of Chemical & Biological Engineering, Iowa State University of Science and Technology, Sweeney Hall, Ames, IA, 50011.

[3] Ames Laboratory, U.S. Department of Energy, Ames, IA, 50011

[4] Department of Chemistry, Life Sciences and Sustainability, University of Parma, Parco Area delle Scienze, 17/A, 43124 Parma, Italy.

[‡] current address: Department of Geography and Environmental Science, The University of Reading, Whiteknights, PO Box 227, Reading, RG6 6AB, UK.

[†] current address: Department of Nutritional Sciences, The Pennsylvania State University, 110 Chandlee Laboratory, University Park, PA 16802

[§] These authors contributed equally to this work

[*] Author to whom correspondence should be addressed: ludovico.cademartiri@unipr.it

Abstract

We hereby show that root systems adapt to a spatially discontinuous pattern of water availability even when the gradients of water potential across them are vanishingly small. A paper microfluidic approach allowed us to expose the entire root system of *Brassica rapa* plants to a square array of water sources, separated by dry areas. Gradients in the concentration of water vapor across the root system were as small as 10^{-4} mM·m^{-1} (~4 orders of magnitude smaller than in conventional hydrotropism assays).

In spite of such minuscule gradients (which greatly limit the possible influence of the well-understood gradient-driven hydrotropic response), our results show that (i) individual roots as well as the root system as a whole adapt to the pattern of water availability to maximize access to water, and that (ii) this adaptation increases as water sources become more rare.

These results suggest that either plant roots are more sensitive to water gradients than humanmade water sensors by 3 to 5 orders of magnitude, or they might have developed, like other organisms, mechanisms for water foraging that allow them to find water in the absence of an external gradient in water potential.

Significance Statement

The supply of water is the most reliable predictor of survival and performance in crops. Nonetheless, our ability to design or breed plants with superior tolerance to drought or flooding is constrained by our limited understanding of how roots adapt to inhomogeneous water supplies.

We here show evidence that roots might not need external gradients in the potential of water to improve their access to it. Our microfluidic apparatus quantified how root systems adapt to

inhomogeneous water supplies while being exposed to gradients in water vapor concentrations that are orders of magnitude smaller than those detectable by some of our best engineered water sensors. We conclude by suggesting possible mechanisms that could explain this behavior.

Introduction

/body

A secure water supply is the strongest predictor of survival in crops(1, 2) and most plants (not all(3)) uptake water mostly from their roots. Therefore, harvesting water is one of the most important, and yet still poorly understood functions of the root system. For example, in spite of great progress(4-11), we still do not fully understand how the architecture of the root system develops to optimize its access to a water supply that is inhomogeneously distributed. Therefore, we have limited information on how to design genomes or select phenotypes that promote, for example, tolerance to drought(4).

The availability of water to plants is usually determined by the water potential (WP), and the hydraulic conductivity (HC) (12). Intuitively, these parameters help quantify respectively how easy is to pull the water (i.e., the lower the WP, the more thermodynamically stable the water is, and the more difficult it is, in general, to change its state), and how rapidly it can be pulled (i.e., the flow of water under a certain pressure differential). These physical parameters can have biological consequences and induce a response: e.g., low water availability can limit the rate of water uptake by the plant and therefore induce water stress. Such limitation on water uptake can be due to the water being too hard to pull, too slow to obtain, and/or too limited in quantity.

Plants can adapt to water scarcity by collecting information about the distribution and availability of water in the surrounding volume of soil and develop the structure of their root system accordingly(13).

Organisms generally “collect information” about their environment by sensing some external potential gradient (e.g., gravitational potential in gravitropism, chemical potential in chemotropism). Therefore, the study of the adaptation of roots to an inhomogeneous water supply has historically focused on understanding how roots grow towards higher WP (i.e., hydrotropism, first reported in 1811(13)). Since 1872, hydrotropism was further investigated by Sachs(14), Molisch(15), Darwin(16), and, more recently, by others(17-21). These recent studies have focused on observing deflections of single roots (22) when exposed to gradients in the potential of water vapor(23) or of the water in the nutrient solution (18).

Nonetheless we were prompted by the observation that in the animal kingdom, foraging is not always guided by sensing of the food source (olfactory, auditory, vision, tactile). Forage can be collected by trapping(24), harvesting(25), luring(26), symbiosis(27), parasitism(28), or its location can be encoded in memory(29) or into a chemical trail(30, 31). These distinct mechanisms allow animals (and some plants(32)) to forage for food sources that cannot be sensed due to their distance, or that move too rapidly to be caught. It is therefore conceivable that plants might have developed one or more mechanisms to seek water in the absence of external gradients of water potential. Therefore we set out to find out.

Experiment Design

Exploring the development of a branched root system in the presence of heterogeneous water availability and in the absence of WP gradients is an experimentally challenging problem. We explain here the design choices that addressed the numerous requirements of such a study.

Analyzing the branched root system of a representative plant. Mechanisms of water foraging that do not involve sensing of an external water potential could rely on the entire root system and might therefore not be observable in single-root assays. Therefore, we designed an experimental habitat in

which a branched root system can be imaged in its entirety.

We chose *Brassica rapa* (Wisconsin Fast Plants® AstroPlants, Carolina®, USA) as a model plant for its fast growth, relatively thick roots that are easy to image, reliably high germination rates, and membership in an economically important family (Brassicaceae).

Removal of the influence of other tropisms on the direction of root propagation. Root systems respond to many stimuli other than water (e.g., gravity, oxygen, nutrients, temperature, light, touch). Isolating the influence of one tropism from the others is notoriously challenging(33, 34).

The effect of gravity on root development (i.e., gravitropism) is especially difficult(35, 36) to remove(35, 37). We constrained the development of roots to a flat, horizontal surface (Figure 1A) (38) to limit the effect of gravity on the direction of root growth(39). Roots are also sensitive to contact with surfaces (i.e., thigmotropism), but our approach ensures that every root tip experiences contact with the same surface roughness and orientation.

Gradients in the concentrations of nutrients and chemicals affect root development (i.e., chemotropism(40)). We ensured that the concentrations of nutrients accessible by the root system (Murashige-Skoog (MS) medium at 0.5X concentration) were constant in time and space by controlling the water transport in the system, as described in a previous publication(41). In short, the plant was grown on what we call the “growth sheet” (Whatman 1 chromatography paper). The growth sheet was placed on top of a stack of paper that was almost completely immersed in a reservoir of nutrient solution (Figure 1A). The concentration of nutrients in the growth sheet was not distinguishable from the one in the reservoir due to the small vertical distance between the two (~1mm). The concentration of nutrients changed little over time because the total amount of nutrients in the reservoir was much larger than the amount consumed by the plant, and evaporation of the reservoir was limited by conducting experiments at high relative humidities (>75%) and was compensated by periodic additions of water (41). Lastly the habitat was sealed and fully autoclaved before use, to avoid the potential

118 influence of microbial contamination (and the potentially associated mechanisms of foraging like
119 symbiosis).

120 Light also affects the direction of root growth as well as the cellular development of the root tissue(34).
121 Therefore, we covered the root system with a slanted sheet of aluminum (Figure 1A). The choice of
122 aluminum was based on its cost, cleanliness, simplicity, and surface chemistry: as the sheet creates a
123 nearly closed environment around the root, condensation can happen on the surface of the sheet that
124 faced the root. This condensation could cause water droplets to bead and drop on the root, thereby
125 changing the distribution of water across the root system. Aluminum's surface is hydrophilic and has
126 small contact and sliding angles for water that cause condensation to drain back into the reservoir
127 (Figure 1A).

128 **Control over gas transport.** The rate of evaporation and plant transpiration is governed by the RH of the
129 atmosphere, the temperature, and by the WP in soil(42). Our laboratory was set to constant
130 temperature (25±1°C) through a redundant air conditioning and ventilation system. We established a
131 homeostatic RH for the plant shoots of 85.0% (SD = 0.77)(38) by placing a supersaturated solution of
132 NaCl inside the plant habitats (Figure 1A). In these conditions, the RH ranged between 75% at the
133 surface of the supersaturated salt solution to ~100% at the surface of the nutrient solution. The shoot
134 lies in between and was therefore exposed to intermediate values of humidity.
135 Aeration is essential to the health of plants. Passive aeration systems (i.e., Parafilm membranes) are
136 ineffective(43). Therefore we actively aerated the habitats with water-saturated sterile air (Figure 1A).
137 **Control over the distribution of water availability in space and time.** Our goal was to test whether the
138 development of the root system is affected by a spatially heterogeneous but temporally constant
139 distribution of water availability, while eliminating the influence of gradients in WP. Since water
140 availability must be modified while maintaining WP constant, the design objective became the spatial
141 control over HC.

It is important to point out that answering our question does not require the spatial control over the absolute values of HC. It only requires the establishment of a binary pattern of HC (i.e., step-wise variations between two constant values), where the low value of HC is sufficiently limiting to water uptake to cause a biological response (e.g., limit plant growth). This point is important because absolute values of HC are difficult to measure reliably: its quantification in our system would have to assume knowledge of the pressure differential caused by the plant in each point of the root system, and the validity of Darcy's law for capillary flow in paper. Both of these assumptions are unwarranted.

We used paper-based microfluidics(44) to solve this problem. In our assay, the flow of nutrient solution to the roots occurs by capillarity: from the reservoir, through the stack of paper sheets underneath the growth sheet, and lastly, through the growth sheet itself (Figure 1B). The HC through the paper stack is determined by the rate of capillary flow. This flow can be hindered (and the HC reduced drastically) by coating the cellulose fibers in the growth sheet with a hydrophobic substance, e.g., wax. This coating can be printed arbitrarily on the growth sheet, thereby designing areas of different HC. The flow of water vapor to the roots is instead unaffected by coating of the cellulose fibers, thereby preventing the establishment of a RH gradient across the root system.

We used a commercially available desktop printer (Xerox Colorqube), to print patterns of wax ink on the top surface of the growth sheet (Figure 1C). Steam autoclaving simultaneously melted the wax and sterilized the paper. As the wax melted, it coated the paper fibers across the entire thickness of the growth sheet, and it spread laterally (Figure 1C). The thickness of a line of wax increased by 1.62 mm as a result of autoclaving, regardless of the original width of the printed line (ALW $=(1.0126\pm0.023)*PLW+(1.62\pm0.12)$, where PLW is the printed line width and ALW is the printed line width after autoclaving), indicating a constant lateral spreading of 0.81 ± 0.06 mm (Figure 1D).

This approach allowed us to create flat supports for root growth where dry areas of negligible HC (i.e., where the wax was printed and molten) and wet areas with high HC (where no wax was printed – we

call these areas “pores” for convenience) were determined with precision, almost as pixels on a screen, and did not change over time.

Figure 1E shows how patterns of pores could be obtained by printing a square grid of wax (we used square patterns for simplicity, but any printable pattern can be chosen). When the autoclaved sheet is placed on a wet reservoir, the pores are filled with water by capillarity (Figure 1F, the water is dyed in red for clarity). The capillary transport of water was effective even for the smallest pores (0.4 mm^2, Figure 1G) and the size of the pores did not affect the local WP (i.e., the pressure required to draw water from the pores): no water was drawn into a capillary in the printed areas, while columns of water of identical height (26 mm at steady state, corresponding to a pressure of 255 Pa) were drawn from pores of different sizes (cf. Supporting Information).

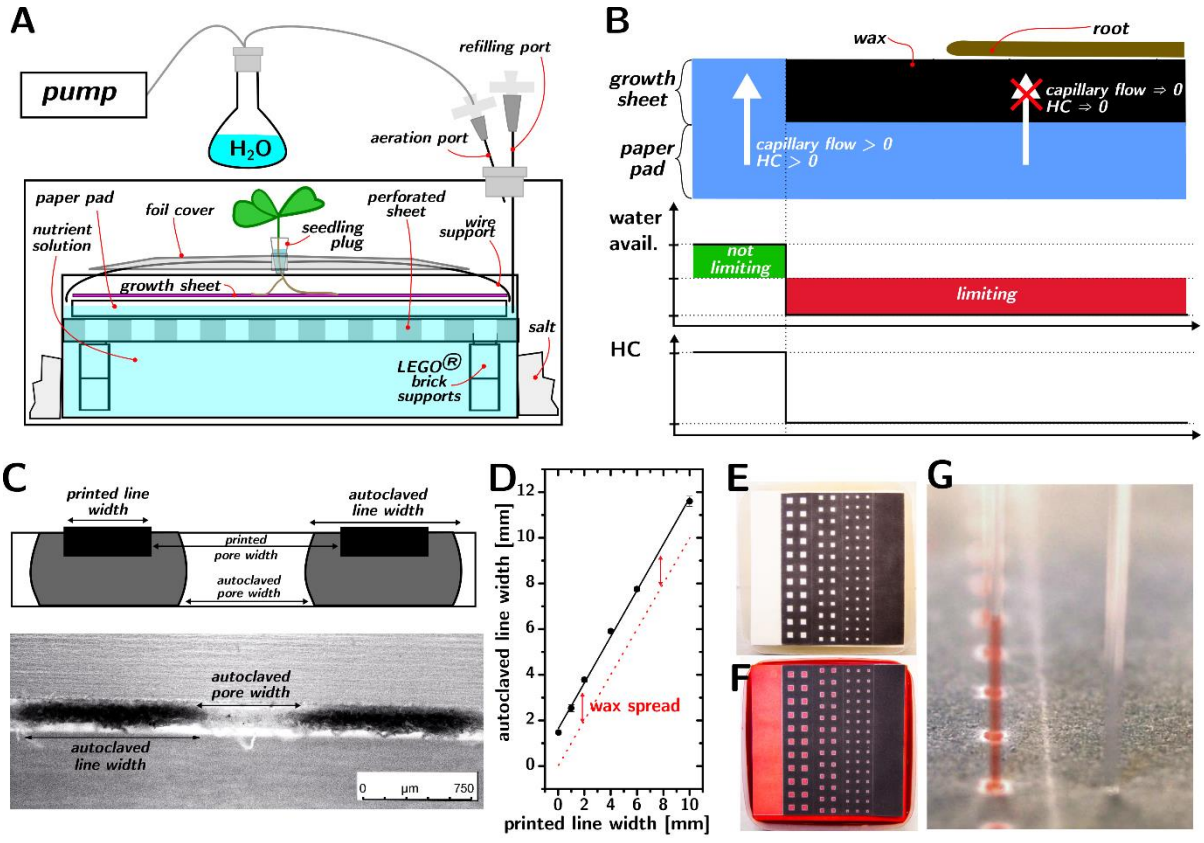

Figure 1. A paper microfluidic assay for studying root development in heterogeneous water availability distributions. A) Schematic representation of the experimental setup; B) Schematic of the control of water availability to the root by the local coating of the growth sheet with wax; C) Schematic and cross-sectional micrograph of wax deposition and diffusion in the paper upon autoclaving; D) Graph of the width of printed line of wax after autoclaving as a function of its width before autoclaving (red dotted line is where the line would be if autoclaving caused no change in the line width); E-F) A square pattern of autoclaved wax on paper before and after being put in contact with red-colored water; G) Comparison of the capillary rise of red-colored water from an unprinted area and a printed area.

The gradient of the liquid WP is assumed to be negligible in the pores and across pores (i.e., nutrient concentration is constant, and the paper is homogeneous in porosity and composition). The liquid WP is also assumed to be negligible across the wax-printed areas as well, where water can exist as an adsorbed interfacial layer (surfaces are coated in a nanoscale layer of water at atmospheric pressure and RH>0, regardless of composition(45)).

Constant humidity across the root system. The availability of liquid water in this system is binary. Therefore, in order to find a pore by sensing water at a distance, a root tip could only follow a gradient of water vapor concentration. Therefore, the gradient of RH across the growth sheet had to be as small as possible (the habitat is outside of thermodynamic equilibrium, so time-averaged gradients in gas concentration cannot be reduced to 0 M/m). The sources and sinks of water vapor in the system are as follows (Figure 2A): the supersaturated salt solution is a sink (75% RH at the liquid/air interface), while the active aeration with saturated air, the evaporation from the paper, and the transpiration from the plant are sources (~100% RH). The humidity between sources and sinks depend on the dominant mechanism of mass transport (convection or diffusion). Our system is actively aerated and

inhomogeneous in temperature (the system is outside of equilibrium so temperature gradients cannot be ruled out) so diffusion only dominates in the boundary layers (i.e., the layer of gas or liquid in contact with a hard surface where convection is negligible). Aeration is very slow (~0.12 m/s) and the Reynolds number is ~24. The Blausius solution for the flow-governing equation(46) predicts a thickness for the boundary layer of ~6 cm, which is much larger than the thickness of the roots (0.2 mm). Therefore, to summarize, the transport of water vapor around the roots in our system is governed by diffusion.

Under these conditions, if the growth sheet contains dry and wet regions, a gradient of water vapor, albeit minuscule, should form across the paper surface: while the air/water interface in the pores is in contact with the root, it is instead recessed by a distance equal to the thickness of the growth sheet in the dry regions (180 μm). This difference in the height of the water/air interface necessarily causes the formation of a gradient in the concentration of water vapor along the growth sheet.

We measured (Figure 2B and Figure S14) the RH above the top surface of the growth sheet (3 mm, the smallest distance we could place our hygrometers from the paper). The lines indicate the increase in RH with time above an unprinted growth sheet (i.e., fully wet, red curve) and a fully printed growth sheet (i.e., fully dry, black curve). The instrumental results show that the RH at steady state is 100% whether the topmost sheet of paper is covered in wax or not. Hence, the gradient in water vapor is much smaller than the precision of our hygrometer.

We therefore conducted a finite-difference time domain (FDTD) simulation to estimate the water vapor concentration in the boundary layer (Figure 2C) with the following assumptions: (i) the problem can be reduced to a 2D diffusion problem, (ii) the distance between the wet paper (source) and the salt solution (sink) is 10 cm, (iii) the wax-coated paper does not limit diffusion of water vapor from the underlying reservoir (supported by the data in Figure 2B), (iv) pores were 0.4 mm^2 in area (to maximize the observed gradients).

The simulation (cf. Supporting Information) captures the decrease in water vapor concentration from the source to the sink (Figure 2C). The concentration profile of water vapor experienced by the root (0.2 mm above the growth sheet) shows peaks in water vapor concentration caused by the pores (Figure 2D, blue trace). The amplitude of the peaks is 1.85 µM and their full width at half maximum (FWHM) is 0.926 ± 0.004 mm. The largest gradient in water vapor concentration (Figure 2D, red trace) is 3.05 $mM \cdot m^{-1}$ located 35 µm from the edge of the pores. In between the pores (i.e., where the root tips conduct most of their growth) the gradients are in the order of 10^{-4} mMm^{-1}. The difference in water vapor concentration across the root tip in such minuscule gradients is ~10^{-11} M. By comparison, the common assay for the study of hydrotropism using salt solutions exposes the root tip to gradients in water concentration that are ten thousand times larger (~1 $mM \cdot m^{-1}$, and differences in concentrations across the root tip of the order of 10^{-7} M).

Furthermore, to reduce the possibility of "false negatives" in the simulations, we conducted them by using boundary conditions that could only *over*estimate the gradients of RH. Most notably, we neglected the presence of the aluminum enclosure. Condensation formed on the surface of the aluminum sheet facing the root during the experiments. The condensed water is a new source of water vapor. Therefore the roots are located between two sources of water vapor, which reduce the gradients of RH within the root volume. Nonetheless, even if the simulations would be incorrect by an order of magnitude, the conclusions of this work would be unaffected.

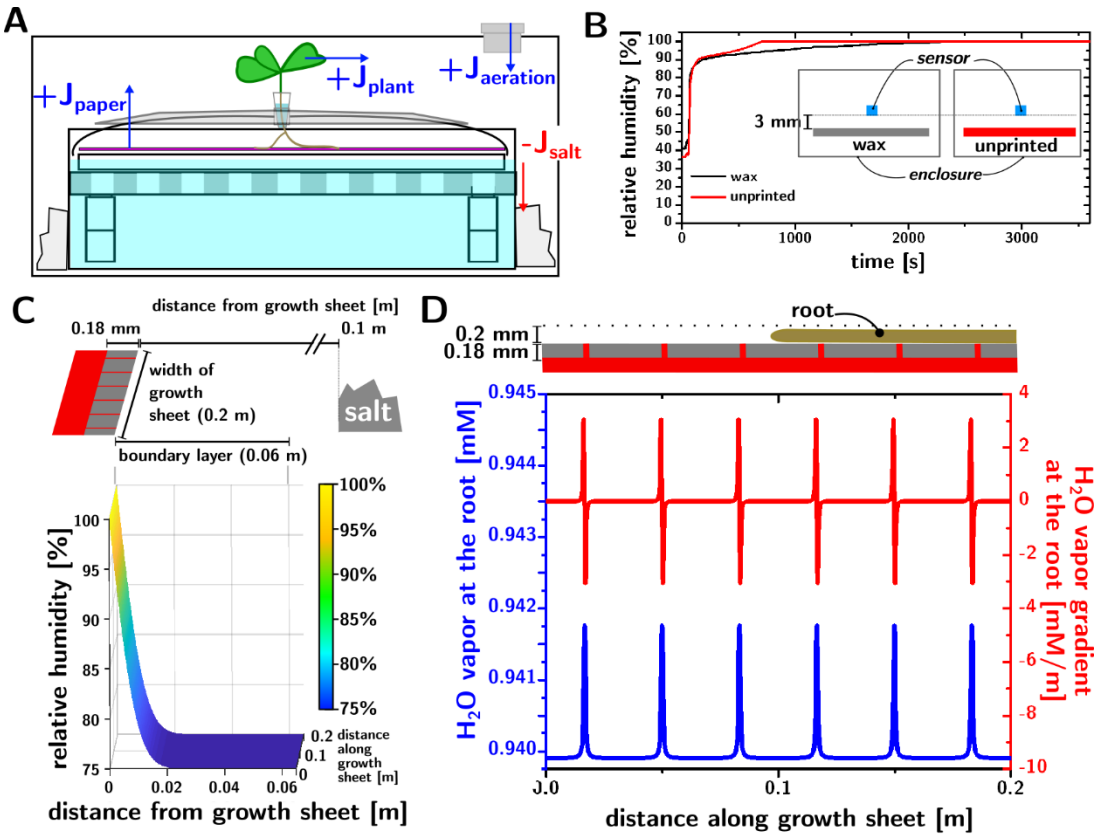

Figure 2. Control and assessment of water vapor gradients. A) Schematic of the setup, highlighting the sources and sinks of water vapor and the directional flows (J) of water vapor at steady state; B) Graph of relative humidity (RH) above a printed (black) and unprinted (red) growth sheet as a function of time, showing the equally fast rise in humidity and saturation at 100% in 1hr; C-D) Simulation of steady state RH above a growth sheet featuring six equally spaced pores. For simplicity, the three-dimensional problem is reduced to two dimensions (a dimension across the growth sheet, and a dimension above the growth sheet). Panel C shows the RH value (vertical axis) as a function of height above the growth sheet (horizontal axis) and the position along the growth sheet (oblique axis), in the presence of printed and unprinted areas. Panel D shows the concentration (in mM, blue) and concentration gradient (in mMm^{-1}, red) of water vapor 0.2 mm above the growth sheet. The horizontal axis indicates the position along the growth sheet.

Results and Discussion

Reducing the wet area reduces the plant biomass. A key requirement for our study was for the water availability in the wax-printed regions to be sufficiently low to limit plant growth. Since the size of

261 the pores do not influence the local availability of water, we quantified the global water availability by
262 the “relative wet area” (RWA), defined as the fraction of the growth sheet surface that was wet.
263 In a square array of square pores, two independent parameters can be used to control the RWA:
264 the printed line width and the printed pore width, as indicated in Figure 1C. The RWA and the area of
265 individual pores as a function of the printed line width and printed pore width were quantified by image
266 analysis (cf. Supporting Information).
267 Plants of *Brassica rapa* were germinated in a system previously described(41) for 5 days (cf.
268 Supporting Information), after which they were transplanted to the setup shown in Figure 1A. There,
269 they were grown at 24-26°C under ~140 PAR ± 10 PAR of illumination for 24 hours/day for 10 days from
270 germination. Plants were grown on growth sheets with 1%, 3%, 6%, 11%, 19% RWA (n = 8, 11, 13, 12,
271 10, respectively, Figure 3A). A 100% RWA treatment (i.e., unprinted growth sheets) was used as a
272 control (n = 20) while the 0% RWA treatment (fully printed growth sheets) led to the nearly complete
273 loss of the plants and could not be considered. The RWA was controlled by the autoclaved pore width
274 (from 0.4 mm for 1% RWA, to 25 mm for 19% RWA, cf. table S1), while the autoclaved line width (ALW)
275 was kept constant (6 mm) so that (i) roots had to cross the same distance of dry surface to reach a new
276 source of water and nutrients regardless of the RWA value, and (ii) the vanishingly small gradient in WP
277 between the pores would be as similar as possible across treatments. The tap roots of the transplanted
278 seedlings were arranged into a “starter” pore (a square of 25 mm^2 in area that was included in all
279 treatments) to ensure high rates of survival for the plants.

280 Root system characterization was conducted at the end of the experiment after excising the stem
281 (Figure 3B). Photographs of the root systems were analyzed to characterize structural root
282 characteristics both in the dry areas as well as in the wet areas (Figure 3C). In summary: (step 1) the
283 background outside of the root system was removed (Figure 3C, panel 1 to 2); (step 2) the pores were
284 cut out of the image due to their different background color and the remaining image was thresholded

285 to yield a binary image of all the roots lying on the wax-coated areas (Figure 3C, panel 2 to 3); (step 3)
286 the roots in the pores were thresholded separately with manual curation, and reinserted in the final
287 image to obtain to complete root system (Figure 3C, panel 3 to 4).

288 Compared to the control treatment (100% RWA), the biomass of both roots and shoots decreased
289 with the RWA (separate control experiments using deionized water as nutrient solution show the
290 biomass to be unaffected, probably due to the young age of the plants, cf. Supporting Information) ,
291 while following an exponential trend of the type

292 $$biomass(RWA) = biomass(RWA=100\%)+A\cdot e^{rate*RWA}$$

293 with a rate equal to -0.062±0.039 (Figure 3D, R^2=0.817). This trend in biomass and the extreme
294 mortality of plants grown at 0% RWA demonstrates that the limitation over HC in the wax-printed areas
295 is sufficient to limit plant growth.

296 A similar trend is observed in the dependence of the root surface area on the RWA (Figure 3E, same
297 exponential trend with a similar rate of -0.055±0.05, R^2=0.817). The root surface area was found to be
298 approximately proportional to the total biomass (Figure 3F, R^2=0.988), suggesting that the average root
299 diameter is similar in all treatments. The convex area of the root system (i.e., defined as the smallest
300 area that is convex and contains the root, Figure 3G, p-value>0.05), and the root surface density (Figure
301 3H, i.e., the ratio between the total surface area of the roots and the convex area of the root system)
302 were not significantly different across treatments.

303 Changes in the architecture of the root system only became apparent after we analyzed *where* the
304 roots were in relation to the pores.

305 ***Roots show a preference for wet regions that increases with their scarcity.*** The most relevant
306 characteristic, which we call “water preference ratio” (WPR) and define as

$$WPR = \frac{\left(\frac{surface\ area\ of\ roots\ on\ pores}{surface\ area\ of\ roots\ on\ wax}\right)}{\left(\frac{pore\ area}{wax\ area}\right)} = \frac{fraction\ of\ pore\ area\ covered\ by\ roots}{fraction\ of\ wax\ area\ covered\ by\ roots}$$

quantifies the ratio of the probabilities of finding a root on a pore and on a dry region. Therefore, if WPR is equal to 1, the probability of finding a root anywhere on the growth sheet is independent of whether that point is wet or dry. If WPR is equal to 2, a wet spot is twice more likely to be covered by a root than a dry spot.

Figure 3I shows the WPR as a function of RWA. Two different curves are shown. The blue scatters show the WPR calculated by considering all pores (i.e., including the starter pore), while the green scatters show the WPR calculated by excluding the starter pore. In both cases the WPR is inversely proportional to the RWA, i.e., WPR = a + b/RWA (a=1.26$\pm$0.44 and b=3.36$\pm$1.16 for the green data set; a=0.62$\pm$0.44 and b=19.10$\pm$1.16 for the blue data set – in both cases the error indicates the 95% confidence interval assuming normally distributed data). The data indicate that, in the absence of water scarcity (i.e., RWA=20%; WPR cannot be calculated for RWA=100%), the roots indicate a weak preference for pores (WPR $\cong$ 1), but this rapidly changes as water becomes more scarce, with the WPR ratio increasing up to ~3.5 or ~15 for RWA=1%, depending on whether the “starter” pore is considered or not.

If we assume that the gradient in WP is too small for the root to detect, the increase in the WPR could be explained by hydropatterning(9, 11, 47): additional branching of the root system on the pores would increase the WPR. We examined the branching points located on pores and found that they only account for ~4% of the total root surface area on the pores: branching on the pores is not responsible for the observed trend in WPR. To confirm this conclusion we looked at the distance between the branching points and the closest pores and found that branching is not overrepresented in the pores nor

328 in their proximity, even for RWA=1% (see Supporting Information S10 and S11). In conclusion, sudden
329 changes in HC do not seem to induce branching in *B. rapa*.

330 The difference in the magnitude of the WPR depending on whether the starter pore is considered
331 or not suggest that water-stressed plants might invest a larger portion of their photosynthate in roots
332 located on known water sources close to the stem and less on roots “scouting” for new water sources.
333 Nonetheless, Figure 3G shows that the convex area was not significantly different among treatments. As
334 a whole, our observations suggest that plants under this kind of water scarcity create a smaller number
335 of “water-scouting” roots, whose length is though unaffected.

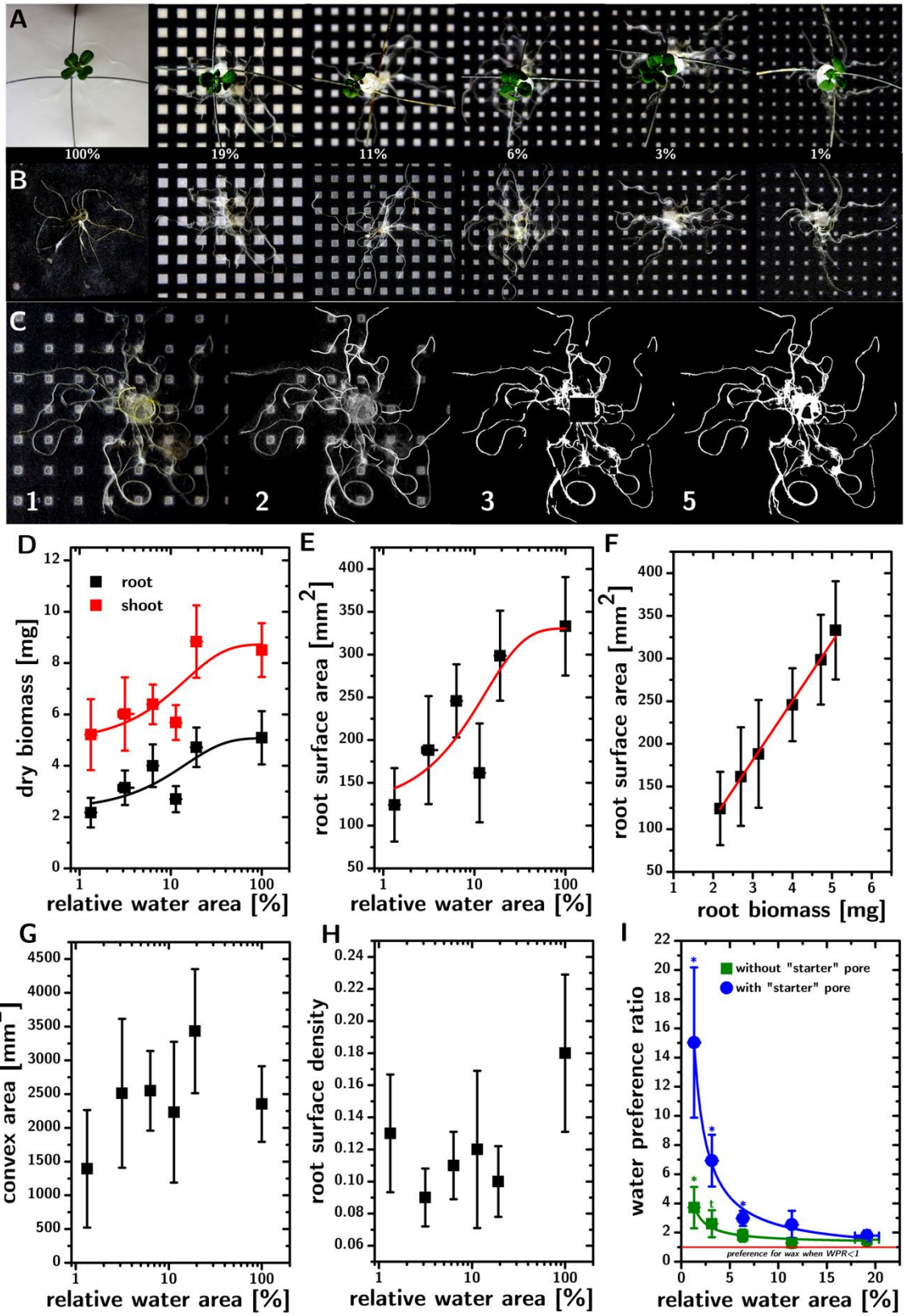
A
100%
19%
11%
6%
3%
1%
B
C
1
2
3
5
D
root
shoot
dry biomass [mg]
relative water area [%]
E
root surface area [mm2]
relative water area [%]
F
root surface area [mm2]
root biomass [mg]
G
convex area [mm2]
relative water area [%]
H
root surface density
relative water area [%]
I
without "starter" pore
with "starter" pore
water preference ratio
preference for wax when WPR<1
relative water area [%]

336

Figure 3 Root and shoot analysis. Representative top-view photographs of plants grown in different relative wet areas (RWA), before (A) and after (B) excising the stem C) Strategy used to extract binary image of the root in 3 steps; D) dry biomass of root (black) and shoot (red) as a function of RWA together with the associated exponential trends (lines). Error bars=95%CI; E) Root surface area as a function of RWA with the associated exponential trend (line). Error bars=95%CI; F) Root surface area as a function of root biomass, showing a straight linear dependence; G) Convex area. Error bars=95%CI. and (H) root surface density as a function of RWA showing lack of significant correlation; Error bars=95%CI. I) Water preference ratio as a function of RWA, calculated by accounting (green squares) or not accounting (blue circles) for the starter pore. Lines indicate reciprocal fits of the data. Error bars=95%CI. Asterisks (*) represent p-value<0.05 while (t) represents a tendency for significance where the p-value<0.08.

The architecture of the whole root system adapts to the position of the water sources.

If the roots seek wet regions, then the overall architecture of the root system should adapt to the distribution of water sources. Furthermore, if the root system architecture is significantly modified by a different spatial distribution of the same amount of water sources, then the position of the water sources must affect the direction in which the roots grow.

We tested this hypothesis by exposing *Brassica rapa* plants (10 days) to two different water distributions (Figure 4A). All treatments consisted of a circular pattern of 8 identical pores surrounding the starter pore (RWA = 0.75 ± 0.04% for both water distributions to ensure water scarcity and a high WPR). However, the distance between the pores and the starter pore was different between treatments (23 mm and 40 mm, n=15 and 19, respectively). We dubbed the two treatments “near” and “far”, respectively. As a control, we conducted the “near” treatment using deionized water as a nutrient medium to infer the potential influence of nutrients and a possible chemotropic explanation for our results. The total root surface area, the root surface area on the pores, root and shoot biomasses were not significantly different for the three treatments (Figure 4B, Table S4). Nonetheless, the convex area in the “far” treatment was 60% larger than for both of the “near” treatments (0.5 MS and DI water; p-value=0.004 and 0.015, Figure 4C), showing that (i) water supplies closer to the stem limited the spread

of the root system, and (ii) that nutrient concentrations do not seem to affect the confining effect of a close water supply.

Given the susceptibility of root convex area to outliers, we confirmed our observations by calculating the surface density of the roots as a function of the distance from the starter pore as determined by the following equation,

$$root\ surface\ density(r) = \frac{\left(\frac{surface\ area\ of\ the\ roots\ (r)}{2\pi r}\right)}{total\ root\ surface\ area}$$

, where *r* is the distance from the starter pore (Figure 4D). The plot confirms that the root in the "near" treatments is more concentrated near the stem than in the far treatment.

Rather than the values for individual distances (cf. Supporting Information), it is more informative to look at the whole distribution. In all treatments the radial root surface density (RSD) can be fitted with a power law ($RSD(r) = A*(r_0-r)^P$, where r_0 is the furthest reach of the roots, *A* is the root surface density at r_0, and *P* is the exponent that quantifies how rapidly the *RSD* decreases with *r*) shown in Figure 4D as lines.

Importantly, the key exponent *P* is not statistically different across "near" treatments (1.99 ± 0.29 and 1.96 ± 0.32), but is very significantly different from in the "far" treatment (1.14 ± 0.25). These results (i) confirm the existence of a root-system-scale adaptation to heterogeneous water availabilities that occurs even with vanishingly small WP gradients, (ii) confirm that this effect is *not* influenced by the concentration of nutrients in the water supply, and (iii) are inconsistent with a "random walk" search algorithm for root system development (which predicts a gaussianly-distributed root surface density).

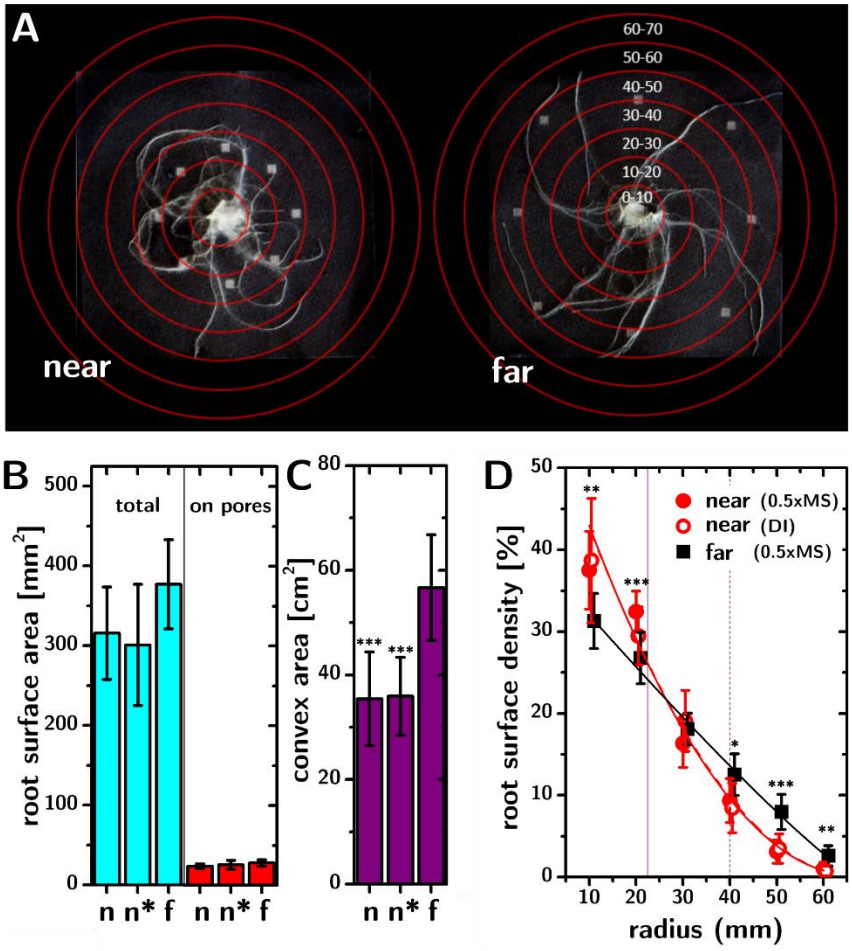

Figure 4. Distribution of water sources controls root architecture. A) Representative top-view photographs of root systems grown in two treatments (both 0.5xMS) with identical relative wet area, but different distance between water sources and the stem ("near", on the left, having pores 23 mm away from the stem, while "far", on the right, having them 40 mm away). B-C) Root surface area, root surface area on pores and convex area of the root systems for "near" treatments (0.5xMS, n, and deionized water media, n*) and "far" treatment (f). The convex area for "near" treatments is significantly lower than in the "far" treatment, ***p-value<0.01. D) Radial root density of the root systems in the "near" and "far" treatments, showing how both "near" treatments have significantly more roots close to the stem than the "far" treatment(*p-value<0.09, **p-value<0.05, ***p-value<0.01). The lines represent power law fits (red solid, red dashed, and black solid for the n, n* and f treatments respectively). The fits for "near" treatments are indistinguishable, but are significantly different from the one for the "far" treatment.

Conclusion

405 We aimed to determine whether plant roots require an external water potential gradient in
406 order to improve their access to water. To this end, we developed a paper microfluidics assay that
407 allowed us to explore the adaptation of entire root systems to a spatially heterogeneous distribution of
408 water availability in a spatially uniform distribution of water potential.

409 Our data show that, in spite of the minuscule gradients of concentration of water vapor (~10^{-4}
410 mMm^{-1}, four orders of magnitude smaller than in the other hydrotropism assays), plants increase their
411 access to water and that their preference for wet regions is inversely proportional to the fraction of the
412 growth surface that was wet. We further showed that the architecture of the root system adapts to the
413 spatial distribution of the wet regions, regardless of the concentration of nutrients in the nutrient
414 solution.

415 We speculate that these results could be explained in at least two equally remarkable ways.
416 Either the roots are capable of sensing differences of water vapor concentrations that are about 3 to 5
417 orders of magnitude smaller than the detection limit of some of our best chemical(48) or optical(49)
418 sensors of water, or, more intriguingly, roots have additional ways to search for water that are not
419 based on responding to *external* gradients in WP. For example, in the absence of WP gradients, a
420 chemical potential gradient could be formed *inside* the root system once a root tip that has been busy
421 responding to other tropism finds water, therefore directing other roots to it.

422 Our approach is distinctly reductionist and it has similarities and differences with soil.
423 Importantly, similarly to soil, the RH at the root system is close to saturation, the availability of liquid
424 water is spatially inhomogeneous, and the roots are kept in the dark. Differently from soil, the roots are
425 constrained in their vertical development (causing them to bunch together at times), are not exposed to
426 significant gradients in temperature, composition (solids, liquids, and gases, notably O_2 and CO_2), and
427 water potential, and are not exposed to interactions with other organisms. Yet, we do not see how the
428 results shown here could be an artifact of these limitations.

We hope that this approach we developed will be useful to other members of the community for (i) studying responses of branched root systems, (ii) identifying new traits and phenotypes associated with tolerance of scarce water, and (iii) rigorously and quantitatively comparing responses to water scarcity in different germplasms.

Materials and Methods

Full details of materials and methods, including the simulation used to assess water vapor gradients, phenotypic root analysis, and system construction, can be found in the SI Appendix. All datasets and images can be accessed using DOI 10.17605/OSF.IO/SQAC3 (52).

Acknowledgments

This work was sponsored by Arnold & Mabel Beckman Foundation through a Beckman Young Investigator Award to LC. We thank Robert Horton for helpful insights. **Competing interests:** The authors declare they have no competing interests. **Author contributions:** LC conceived the project and the experimental design. KRL & OS conceived and conducted the experiments. TS & HV conducted early testing and troubleshooting of the paper microfluidic approach. BY helped the data analysis. SB helped with experiments in low nutrient concentrations. LC performed the diffusion simulations. LC, KRL and OS wrote the paper.

References

1. Comas L, Becker S, Cruz VMV, Byrne PF, & Dierig DA (2013) Root traits contributing to plant productivity under drought. *Frontiers in plant science* 4:442.
2. Turral H, Burke J, & Faurès J-M (2011) *Climate change, water and food security* (Food and Agriculture Organization of the United Nations (FAO)).
3. Rundel P (1982) Water uptake by organs other than roots. *Physiological plant ecology II*, (Springer), pp 111-134.
4. Rogers ED & Benfey PN (2015) Regulation of plant root system architecture: implications for crop advancement. *Curr. Opin. Biotechnol.* 32:93-98.
5. Morris EC*, et al.* (2017) Shaping 3D root system architecture. *Curr. Biol.* 27(17):R919-R930.
6. Scharwies JD & Dinneny JR (2019) Water transport, perception, and response in plants. *J. Plant Res.*:1-14.

7. Orman-Ligeza B*, et al.* (2018) The xerobranching response represses lateral root formation when roots are not in contact with water. *Curr. Biol.* 28(19):3165-3173. e3165.
8. Yu P, Hochholdinger F, & Li C (2019) Plasticity of lateral root branching in maize. *Frontiers in plant science* 10.
9. Orosa-Puente B*, et al.* (2018) Root branching toward water involves posttranslational modification of transcription factor ARF7. *Science* 362(6421):1407-1410.
10. Yu P, Gutjahr C, Li C, & Hochholdinger F (2016) Genetic control of lateral root formation in cereals. *Trends Plant Sci.* 21(11):951-961.
11. Bao Y*, et al.* (2014) Plant roots use a patterning mechanism to position lateral root branches toward available water. *Proceedings of the National Academy of Sciences* 111(25):9319-9324.
12. Ritchie J (1981) Soil water availability. *Plant Soil* 58(1):327-338.
13. Knight TA (1811) XI. On the causes which influence the direction of the growth of roots. By TA Knight, Esq. FRS In a letter to the Right Hon. Sir Joseph Banks, Bart. KBPR S. *Philosophical Transactions of the Royal Society of London* 101:209-219.
14. Sachs J (1887) *Lectures on the Physiology of Plants* (Clarendon Press).
15. Molisch H (1884) *Untersuchungen über den Hydrotropismus*.
16. Darwin C (1897) *The power of movement in plants* (Appleton).
17. Dietrich D*, et al.* (2017) Root hydrotropism is controlled via a cortex-specific growth mechanism. *Nature plants* 3(6):17057.
18. Antoni R, Dietrich D, Bennett MJ, & Rodriguez PL (2016) Hydrotropism: analysis of the root response to a moisture gradient. *Environmental Responses in Plants*, (Springer), pp 3-9.
19. Cassab GI, Eapen D, & Campos ME (2013) Root hydrotropism: an update. *American journal of botany* 100(1):14-24.
20. Takahashi H (1997) Hydrotropism: the current state of our knowledge. *Journal of plant research* 110(2):163.
21. Eapen D, Barroso ML, Ponce G, Campos ME, & Cassab GI (2005) Hydrotropism: root growth responses to water. *Trends Plant Sci.* 10(1):44-50.
22. Dietrich D (2018) Hydrotropism: how roots search for water. *J. Exp. Bot.* 69(11):2759-2771.
23. Moriwaki T, Miyazawa Y, Kobayashi A, & Takahashi H (2013) Molecular mechanisms of hydrotropism in seedling roots of Arabidopsis thaliana (Brassicaceae). *Am. J. Bot.* 100(1):25-34.
24. Nyffeler M, Sterling W, & Dean D (1994) How spiders make a living. *Environ. Entomol.* 23(6):1357-1367.
25. Nørgaard T & Dacke M (2010) Fog-basking behaviour and water collection efficiency in Namib Desert Darkling beetles. *Frontiers in zoology* 7(1):23.
26. Crozier W (1985) Observations on the food and feeding of the angler-fish, Lophim piscatorius L., in the northern Irish Sea. *J. Fish Biol.* 27(5):655-665.
27. Dean W & MacDonald I (1981) A review of African birds feeding in association with mammals. *Ostrich* 52(3):135-155.
28. Pietsch TW (2005) Dimorphism, parasitism, and sex revisited: modes of reproduction among deep-sea ceratioid anglerfishes (Teleostei: Lophiiformes). *Ichthyol. Res.* 52(3):207-236.
29. Polansky L, Kilian W, & Wittemyer G (2015) Elucidating the significance of spatial memory on movement decisions by African savannah elephants using state–space models. *Proceedings of the Royal Society B: Biological Sciences* 282(1805):20143042.
30. Sumpter DJ & Beekman M (2003) From nonlinearity to optimality: pheromone trail foraging by ants. *Anim. Behav.* 66(2):273-280.
31. Tweedy L*, et al.* (2020) Seeing around corners: Cells solve mazes and respond at a distance using attractant breakdown. *Science* 369(6507).

32. Yoshida S & Shirasu K (2012) Plants that attack plants: molecular elucidation of plant parasitism. *Curr. Opin. Plant Biol.* 15(6):708-713.
33. Poorter H & Nagel O (2000) The role of biomass allocation in the growth response of plants to different levels of light, CO2, nutrients and water: a quantitative review. *Funct. Plant Biol.* 27(12):1191-1191.
34. Kiss JZ, Mullen JL, Correll MJ, & Hangarter RP (2003) Phytochromes A and B mediate red-light-induced positive phototropism in roots. *Plant Physiol.* 131(3):1411-1417.
35. Morohashi K*, et al.* (2017) Gravitropism interferes with hydrotropism via counteracting auxin dynamics in cucumber roots: clinorotation and spaceflight experiments. *New Phytol.* 215(4):1476-1489.
36. Takahashi N, Yamazaki Y, Kobayashi A, Higashitani A, & Takahashi H (2003) Hydrotropism interacts with gravitropism by degrading amyloplasts in seedling roots of Arabidopsis and radish. *Plant Physiol.* 132(2):805-810.
37. Takahashi N, Goto N, Okada K, & Takahashi H (2002) Hydrotropism in abscisic acid, wavy, and gravitropic mutants of Arabidopsis thaliana. *Planta* 216(2):203-211.
38. Sizmur T, Lind KR, Benomar S, VanEvery H, & Cademartiri L (2014) A Simple and Versatile 2-Dimensional Platform to Study Plant Germination and Growth under Controlled Humidity. *PLoS One* 9(5):e96730.
39. Ge L & Chen R (2016) Negative gravitropism in plant roots. *Nature plants* 2(11):16155.
40. Hodge A (2004) The plastic plant: root responses to heterogeneous supplies of nutrients. *New Phytologist* 162(1):9-24.
41. Lind KR*, et al.* (2016) Plant Growth Environments with Programmable Relative Humidity and Homogeneous Nutrient Availability. *PloS one* 11(6):e0155960.
42. Martínez-Vilalta J, Poyatos R, Aguadé D, Retana J, & Mencuccini M (2014) A new look at water transport regulation in plants. *New Phytol.* 204(1):105-115.
43. Banerjee S*, et al.* (2019) Stress response to CO2 deprivation by Arabidopsis thaliana in plant cultures. *PLoS One* 14(3):e0212462.
44. Carrilho E, Martinez AW, & Whitesides GM (2009) Understanding Wax Printing: A Simple Micropatterning Process for Paper-Based Microfluidics. *Anal. Chem.* 81(16):7091-7095.
45. James M*, et al.* (2011) Nanoscale condensation of water on self-assembled monolayers. *Soft Matter* 7(11):5309-5318.
46. Schlichting H & Gersten K (2016) *Boundary-layer theory* (Springer).
47. Robbins NE & Dinneny JR (2015) The divining root: moisture-driven responses of roots at the micro-and macro-scale. *J. Exp. Bot.* 66(8):2145-2154.
48. Ooyama Y, Furue K, Uenaka K, & Ohshita J (2014) Development of highly-sensitive fluorescence PET (photo-induced electron transfer) sensor for water: anthracene–boronic acid ester. *RSC Advances* 4(48):25330-25333.
49. Rieker G*, et al.* (2007) A diode laser sensor for rapid, sensitive measurements of gas temperature and water vapour concentration at high temperatures and pressures. *Meas. Sci. Technol.* 18(5):1195.